Rapid Communications

Transformable ferroelectric control of dynamic magnetic permeability

Changjun Jiang, Chenglong Jia,* Fenglong Wang, Cai Zhou, and Desheng Xue†
Key Laboratory for Magnetism and Magnetic Materials of MOE, Lanzhou University, Lanzhou 730000, China and School of Physics Science and Technology, Lanzhou University, Lanzhou 730000, China

(Received 31 July 2017; published 23 February 2018)

Magnetic permeability, which measures the response of a material to an applied magnetic field, is crucial to the performance of magnetic devices and related technologies. Its dynamic value is usually a complex number with real and imaginary parts that describe, respectively, how much magnetic power can be stored and lost in the material. Control of permeability is therefore closely related to energy redistribution within a magnetic system or energy exchange between magnetic and other degrees of freedom via certain spin-dependent interactions. To avoid a high power consumption, direct manipulation of the permeability with an electric field through magnetoelectric coupling leads to high efficiency and simple operation, but remains a big challenge in both the fundamental physics and material science. Here we report unambiguous evidence of ferroelectric control of dynamic magnetic permeability in a Co/Pb$(Mg_{1/3}Nb_{2/3})_{0.7}Ti_{0.3}O_3$ (Co/PMN-PT) heterostructure, in which the ferroelectric PMN-PT acts as an energy source for the ferromagnetic Co film via an interfacial linear magnetoelectric interaction. The electric field tuning of the magnitude and line shape of the permeability offers a highly localized means of controlling magnetization with ultralow power consumption. Additionally, the emergence of negative permeability promises a new way of realizing functional nanoscale metamaterials with adjustable refraction index.

DOI: 10.1103/PhysRevB.97.060408

It is often assumed that it is not possible to alter the characteristic magnetic permeability of a material once the material has been prepared; for instance, zero and negative magnetic permeability are specific to superconductors [1–4] and metamaterials, respectively [5–8]. One can also easily distinguish between ferromagnets, paramagnets, and diamagnets based on their relative (static) permeability. In the practical use of magnetic properties, the magnetization dynamics are governed by the complex dynamic permeability [9–11] $\mu = \mu' + i\mu''$; μ' determines the reorientation angle of the magnetization processional mode, whereas the processional damping is solely dependent on the imaginary part μ''. Large μ' and μ'' suggest a small magnetization switching field and a short magnetization relaxation time, respectively. In particular, a *negative* μ'' and thus a negative damping phenomenon is highly welcome in magnetism, since it allows one to switch the magnetization fast and energetically. However, most of the work carried out so far in this field has been to realize the control of permeability by a change of ferromagnetic resonance (FMR) frequency (or resonant field) via effective magnetic fields—for instance, electric field induced effective magnetic anisotropy [12]—while having no influence on the line shape of dynamic permeability. Consequently, one can have only a shift of the resonance frequency, but μ'' is still positive and the line shape of permeability keeps the standard Lorentzian aspect. Continuous and full control of permeability (including its magnitude and even the line shape) is therefore very desirable for high density magnetic information storage and spintronic devices. On the other hand, together with the electric permittivity ε, the dynamic magnetic permeability μ also determines the refractive index $n = (\varepsilon\mu)^{1/2}$ of the electromagnetic properties of a material. A tunable μ, especially a negative real part μ' and then negative refraction, therefore also represents a great potential to control electromagnetic wave propagation performance, which would open up new perspectives in optimizing materials for optical devices.

From an energy point of view, one promising approach to steer magnetic permeability is to connect magnetization dynamics with an external energy source or drain. Experimentally, this can be realized with an appropriately integrated ferromagnetic (FM) film with proper adjacent substrate. One example that has been studied extensively is the FM/normal-metal (NM) structure. Magnetization precession in the FM film produces a spin current that flows into the NM system [13], which provides an additional energy transfer route to the FM and results in enhanced magnetization processional damping and thus permeability (μ''). Conversely, by injecting a spin polarized current through the interface into the FM film [14,15], such as in the case of a trilayer FM_1/NM/FM_2 tunneling junction, a negative damping torque on the FM_2 could be obtained owing to the selective scattering of injected electrons in the minority channel [16–19]. Such an enhancement and negative damping are very helpful for fast magnetization switching; however, they require high electric current densities, on the order of 10^{10}–10^{12} A m^{-2}, which can be a serious problem especially in nanoscale magnetic structures because of Ohmic dissipation.

What will happen if we interface an FM film with an insulating ferroelectric (FE) substrate? Could full control of magnetic permeability by an electric field rather than a high power electric current be achieved? Given the absence of time-reversal and space-inversion symmetries at the FM/FE

*cljia@lzu.edu.cn
†xueds@lzu.edu.cn

interface, the two ferroic (magnetic and electric) order parameters could be cross-coupled [20,21]. This would introduce the excitations triggered by an electric field to the spin system directly, leading to FE changes in the magnetization and its dynamics. Suppose we have a linear magnetoelectric (ME) coupling at the FM/FE interface. The induced magnetization δm_i by applying microwave field is

$$\delta m_i = \chi^m_{ii} h_i + \frac{\alpha_{ji}}{\mu_0} e_j, \tag{1}$$

where α is the ME tensor. $\chi^m = \mu - 1$ is the intrinsic magnetic susceptibility in the FM subsystem. h and e are the ac magnetic field and electric field, respectively, satisfying the Maxwell-Faraday equation $\nabla \times e = -\frac{1}{\mu}\frac{\partial \boldsymbol{h}}{\partial t}$, which reconstitutes the magnetic/electric field codriven *effective* dynamic magnetic susceptibility $\tilde{\chi}^m$ [22],

$$\mathrm{Im}[\tilde{\chi}^m] = \beta \mathrm{Im}[\chi^m]\cos\phi + \beta \mathrm{Re}[\chi^m]\sin\phi, \tag{2}$$

$$\mathrm{Re}[\tilde{\chi}^m] = \beta \mathrm{Re}[\chi^m]\cos\phi - \beta \mathrm{Im}[\chi^m]\sin\phi, \tag{3}$$

where $\mathrm{Re}[\chi^m]$ and $\mathrm{Im}[\chi^m]$ are the real and imaginary parts, respectively, of the *intrinsic* magnetic susceptibility χ^m of FM material without ME interactions. $\beta e^{i\phi} = (1 + \frac{\alpha c}{n})$, in which the phase ϕ between the induced magnetization and the applied ac magnetic field is mainly due to the complex refractive index n of the FM subsystem, but its value is determined by the ratio $\alpha c/n$. For the case when linear ME interaction $\alpha = 0$ one has $\phi = 0$ and $\beta = 1$, which returns to the magnetic susceptibility in natural isolated FM systems. However, the comparable real and imaginary parts of the complex refractive index ($|n| \sim 10^3$) of typical FM metals (Fe, Co, and their alloys at 140 GHz) [23] and the large ME coupling ($\alpha \sim 10^{-7}$ s/m) at the FM/FE interface could result in nontrivial phase ϕ and considerable modification of the effective magnetic susceptibility $\tilde{\chi}^m$ in the GHz range. In particular, considering that the real ($\mathrm{Re}[\chi^m]$) and imaginary ($\mathrm{Im}[\chi^m]$) parts of natural FM under microwave irradiation normally demonstrate themselves as a dispersive and an absorptive Lorentzian line shape with the frequency of the applied microwave field, such nontrivial phase ϕ would trigger a mixture of the dispersive and absorptive modes in the FM subsystem, resulting in a transformable magnetic permeability $\tilde{\chi}^m$ provided that ϕ is ferroelectrically tunable. This transformable behavior of the dynamic permeability is not only the *general* but also the *unique* feature of experimental linear ME systems.

In FM/FE heterostructures generally, however, (butterfly) strain and (linear) charge mediated ME effects are both expected at the FM/FE interface. Such coexistence would make it very difficult to quantitatively distinguish these two magnetoelectric coupling mechanisms. A promising way for this purpose is to investigate the dynamic magnetoelectric response, particularly the resonance dynamics induced by *only* microwave fields in the GHz range, in which case the interfacial strain has nearly no change and the direct charge-mediated *linear* ME interaction can be emphasized by the collective excitation modes.

Experimentally, to investigate such interfacial ME dynamic effects in FM/FE heterostructures, Co/PMN-PT was fabricated by magnetron oblique sputtering of polycrystalline Co film on PMN-PT (011) single crystalline substrates. Co thin films were deposited on a PMN-PT (011) (thickness of 400 μm) substrate by radio frequency magnetron sputtering. The background pressure was lower than 5×10^{-5} Pa. For the deposition of Co layers, a Co target 75 mm in diameter and 3 mm in thickness was used as the sputtering target, and argon gas was used as the ambient gas. The sputtering chamber was evacuated to a base pressure of 0.2 Pa. The RF power was 50 W. The thickness of the deposited Co layer was 20 nm. The oblique sputtering angle of the film was 20° without an applied field. It is worth emphasizing that the easy axis of the film was perpendicular to the [0 1 −1] direction of the substrate. During sputtering, the temperature of the substrate was maintained at 200 °C to improve the interface between the Co and PMN-PT. Subsequently, 50 nm Pt layers were sputtered on both the top and bottom sides of the Co/PMN-PT structure by magnetron sputtering at room temperature to serve as electrodes. The microwave permeability of the films was measured with a vector network analyzer (PNA E8363B) using a microstrip method [24]. Compared with the reference Co/Si system, the piezoelectric effect in the PMN-PT would in principle give rise to combined strain-mediated [12,25] and (screening) charge-mediated [26,27] ME interaction at the interface. However, the interfacial strain-mediated coupling has an indirect and nonlinear effect on the FM. To emphasize the direct/linear ME effect driven by the screening effect, an in-plane uniaxial magnetic anisotropy $\mathbf{H}_a$ of the Co film was designed along the [0 1 −1] direction of the PMN-PT substrate [Fig. 1(a)]. In this geometry, the effective magnetic field arising from the interfacial strain-mediated ME interaction via piezoelectricity and magnetostriction is associated with an additional contribution to the magnetic anisotropy $\mathbf{H}_a$ along the same direction [28,29]. Ignoring tiny modifications of the lattice parameter by changes in the interfacial stress, it is easily found that the strain-mediated ME interaction alters only the position of the resonant frequency of μ but cannot cause phase mixture and has no direct influence on the line shape of the permeability. However, the electric neutrality constraint at the interface implies that the screening charge density, $\sigma = \varepsilon E$, at the Co surface can be substantially enhanced by the application of dc/ac electric field E because of the large dielectric permittivity of PMN-PT ($\varepsilon \approx 4$–6×10^3) [30]. Furthermore, the screening electrons are spin-polarized owing to the *s-d* exchange interaction with the local ferromagnetic moments, and their spin diffusion in the FM subsystem results in a strong ME interaction at the interface on the nanometer scale, determined by the spin diffusion length (38 ± 12 nm in Co), as shown in Fig. 1(b). Such an interfacial ME coupling brings the FE polarization dynamics into direct and linear contact with the magnetization dynamics. Subsequently, magnetic/electric field codriven magnetization dynamics are obtained, giving rise to a transformable dynamic permeability of the Co with FE tuning of phase ϕ as discussed above.

Figsures 1(c) and 1(d) show the frequency (ω) dependence of the dynamic permeability of Co/Si and Co/PMN-PT systems, respectively, under applied microwave magnetic field **h** along the magnetic hard axis (HA). We note that (1) In the reference Co/Si heterostructure without any ME coupling [Fig. 1(c)], the frequency dependence of real part of dynamic

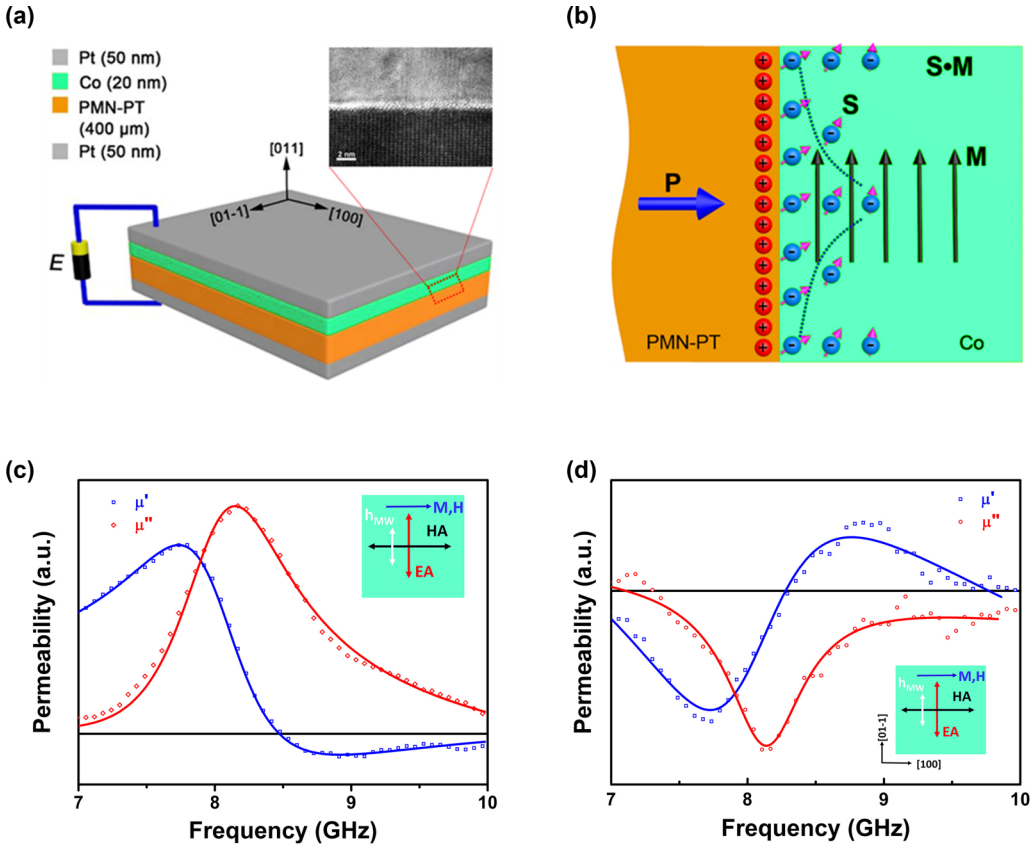

FIG. 1. (a) Sketch of Co/PMN-PT heterostructure and Pt electrodes. Inset: high resolution transmission electron microscopy image of interface between Co and PMN-PT. (b) Illustration of spin-polarized screening at the interface. Interfacing Co with PMN-PT triggers an exponential spiral spin density in the Co within the spin-diffusion length. **P** indicates the FE polarization in PMN-PT. (c) HA dynamic permeability of the Co layer on the Si substrate against the frequency of the microwave magnetic field. (d) HA dynamic permeability of the Co layer on the PMN-PT substrate against the frequency of the microwave magnetic field. The real and imaginary parts of the permeability are represented by squares and circles, respectively. Inset: Directions of the applied dc magnetic field **H** (550 Oe), applied microwave magnetic field **h**, and magnetization $\mathbf{M}_s$ of the Co layer.

permeability shows mostly as a (Lorentzian) dispersive-type line shape and the imaginary part demonstrates itself as a (positive) absorptive-type line shape, which is very similar to the well-established case of isolated ferromagnets; (2) in the Co/PMN-PT system [Fig. 1(d)], however, we observed an anomalous behavior of the permeability's line shape even in the absence of gate voltage. Both $\mu'(\omega)$ and $\mu''(\omega)$ of Co/PMN-PT exhibited large distortion and became not a pure Lorentzian-type signal but a superposition of the dispersive and absorptive modes. Particularly, as shown in Fig. 1(d), $\mu'(\omega)$ and $\mu''(\omega)$ all changed to negative values at low frequency. This is very uncommon, since $\mu'(\omega)$ is usually positive (*negative*) in the region below (*above*) the resonance frequency and $\mu''(\omega)$ shows always positive absorption signal [cf. also Fig. 1(c)]. In practice, however, it is important because $\mu' < 0$ is the condition necessary for achieving negative refraction index metamaterials, and $\mu'' < 0$ with negative magnetic damping is highly desirable for fast switching of the magnetization.

To obtain more insight into the effects of the interfacial ME on the magnetization dynamics and mixture phase ϕ, the imaginary permeability/susceptibility ($\mu'' = \mathrm{Im}[\tilde{\chi}^m]$) was investigated in detail under different polarization **P** and magnetization **M** via the more direct and sensitive ferromagnetic resonance (FMR) spectroscopy in a JEOL JES-FA 300 (X-band at 8.969 GHz) spectrometer (sketches of the sample and the measurement configuration are shown in Figs. S5(a) and S5(b) of the Supplemental Material [31]). The microwave power, $\wp(h)$, absorbed by the Co film in the FMR measurements is given by $\wp(h) = \omega \mathrm{Im}[\tilde{\chi}^m]|h|^2/2$, from which the imaginary susceptibility $\mathrm{Im}[\tilde{\chi}^m]$ can be directly deduced. Figure 2 presents the obtained FMR spectra of the Co/PMN-PT heterostructure in the cases of static electric field being absent. For the as-fabricated unpoled PMN-PT substrate with average FE polarization $\langle \mathbf{P} \rangle = 0$, the static screening charges induced by the FE polarization were zero and the piezoelectric strain vanished as well. Only dynamic screening driven by the microelectric field plays a role in the interfacial ME effect. Compared with the Si substrate, the main difference is that the large permittivity of PMN-PT can magnify this dynamic ME effect at the Co/PMN-PT interface. From the uniaxial symmetry of the polycrystalline Co film, we expect that the magnetic permeability should have twofold rotational symmetry; it follows that the refractive index n and thus the phase ϕ would possess C_{2v} symmetry as well via the linear dynamic ME effect. Such a distinctive anisotropic feature of the phase ϕ was confirmed in the experimental observations for

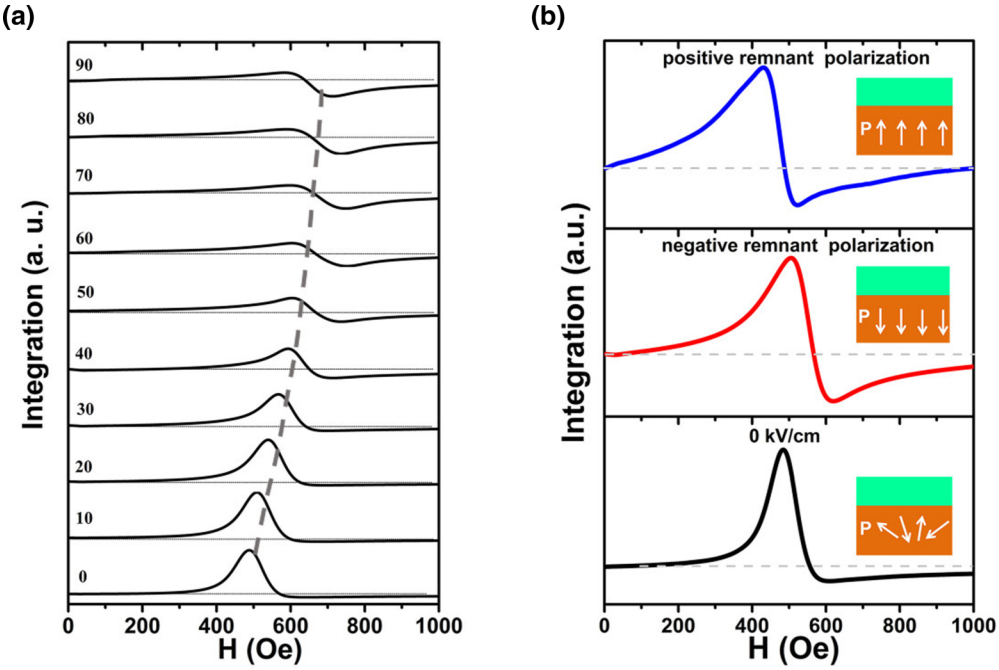

FIG. 2. (a) Integrated power derivative against in-plane magnetic field H at different angles with respect to the EA direction. The microwave magnetic field was normal to the film plane. The static electric field is absent, and the FE PMN-PT substrate is unpoled. (b) Integrated power derivative against in-plane magnetic field H at different prepolarization states with respect to the EA direction.

unpoled PMN-PT by rotating the in-plane dc magnetic field H, asV demonstrated in Figs. 2(a) and 3(a). It indicates that the dielectric permittivity and magnetic permeability of FM/FE system, other than the magnetic moment and electric polarization [19,21], are also crucial to the dynamic ME response of multiferroic FM/FE heterostructures. On the other hand, concerning the static screening effect caused by the nonvanishing normal polarization $\langle \mathbf{P} \rangle$, we note that the FMR spectra of unpoled Co/PMN-PT with $\langle \mathbf{P} \rangle = 0$ possessed a normal (positive) absorptive Lorentzian shape when the dc magnetic field H was applied along the easy axis (EA) direction [cf. Fig. 2(b)]; however, its line shape dramatically changed as PMN-PT was FE polarized as $\langle \mathbf{P} \rangle \neq 0$, and a negative signal emerges above the FMR frequency under the dc electric field $E = 0$ ([cf. Fig. 2(b)]. Furthermore, the ferroelectric control of the polarization $\langle \mathbf{P} \rangle$ allowed us to continuously tune the FMR spectra by applying dc electric field E. Taking the magnetic susceptibility χ^m of Co/Si heterostructures (Fig. S5(c) [31]) as a reference frame, the deformed susceptibility $\mathrm{Im}(\tilde{\chi}^m)$ of Co/PMN-PT was found to be fitted quite well by the theoretical formula (2), where the mixture phase ϕ is dc electric field dependent owing to the ferroelectric tuning of the ME coupling tensor α [cf. Fig. 3(b)]. Several interesting and important phenomena occur: $\mathrm{Im}(\tilde{\chi}^m) \approx -\mathrm{Im}[\chi^m]$ is realized when $\phi \approx \pi$ at $E = \pm 10$ kV/cm; a completely negative imaginary susceptibility and thus negative magnetization damping are obtained. Second, for the two limiting cases around $E = 0$ and $E = \pm 15$ kV/cm, $\phi \approx \pi/2$ and $3\pi/2$, respectively, and the line shape of the effective imaginary susceptibility totally changes from an absorptive to a dispersive Lorentzian line ($\mathrm{Im}(\tilde{\chi}^m) \approx \pm \mathrm{Re}[\chi^m]$), which is associated with the strongly suppressed magnetization procession damping around the resonant magnetic field. Finally, given the vanishing of the piezoelectric strain in both unpoled and poled PMN-PT substrates under applied electric field $E = 0$, the deformed line shape of the FMR spectra with $E = 0$ intrinsically rules out a possible contribution from the strain-mediated ME coupling. From the above discussion, we can further conclude that the observed transformable behavior originated from the direct electric field effect at the FM/FE interface, and that the linear ME interaction is crucial for the ferroelectric control of magnetic permeability.

It is, however, challenging and difficult to subtract the possible contributions of FE dynamics from the FMR absorption signals. A promising way for this clarification is to directly measure magnetic permeability spectra. Given that the refractive index n is frequency dependent, which implies that the phase ϕ should also vary with resonance frequency. Correspondingly, both the real and the imaginary parts of magnetic permeability/susceptibility should evolve according to Eqs. (2) and (3). In Fig. 4, the frequency dependence of the dynamic permeability under various applied dc magnetic fields is shown for PMN-PT substrate under positive remnant polarization by a vector network analyzer with the microstrip method. With increasing dc magnetic fields H, the resonance frequency followed the Kittel formula. The real and the imaginary permeabilities of Co/Si were found to keep almost the same line shape without deformation [cf. Figs. 4(c) and 4(d). At low H, Co/PMN-PT showed a normal dynamic permeability spectrum. However, as demonstrated in Figs. 4(a) and 4(b), the two most obvious changes are the line shape and the value of the dynamic permeability of the Co/PMN-PT with increasing . By $H = 200$ Oe, the real permeability was driven to become negative. When H was further increased above 550 Oe, both the real and imaginary dynamic permeabilities became completely negative. This remodeling of permeability is consistent with the FMR

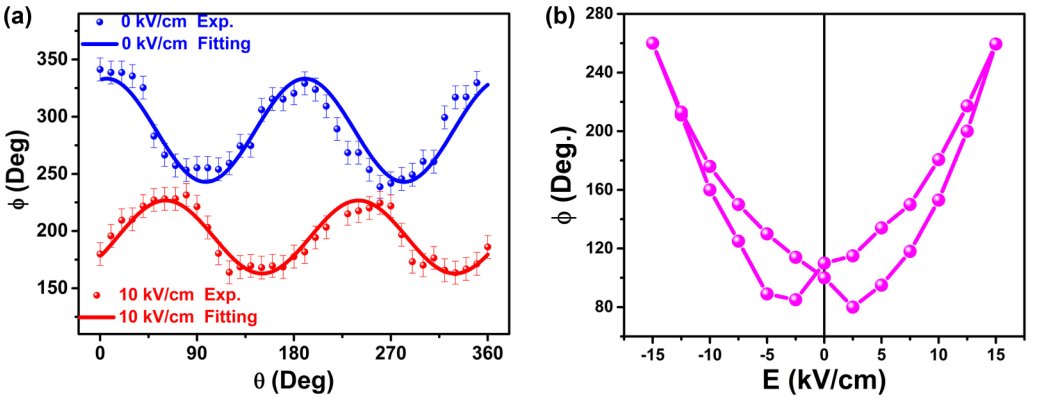

FIG. 3. (a) Change in mixture phase ϕ with angle between the static magnetic field H and magnetization easy axis under unpoled state and $E = 10\,\mathrm{k\,V/cm}$. Solid lines show fitting curves with introduced C_{2v} symmetry. (b) Change in mixture phase ϕ with electric field E applied normally to the Co/PMN-PT.

observations and satisfies the dynamic ME effect [Eq. (2)] as well: The real part continuously changed from a Lorentzian dispersive shape to an absorptive shape, while the imaginary part showed the opposite. The fitted phase ϕ decreased linearly with the applied magnetic field H. As the dc magnetic field H was changed, the S_{11} of the PMN-PT substrate remained unchanged as shown in Fig. S6 [31], which excludes the effect of the dielectric permittivity of the substrate and illustrates that the linear interface ME interaction indeed plays a dominant role in the transformable magnetic permeability.

The present demonstration of linear ME coupling as an energy transfer intermediary at the Co/PMN-PT interface

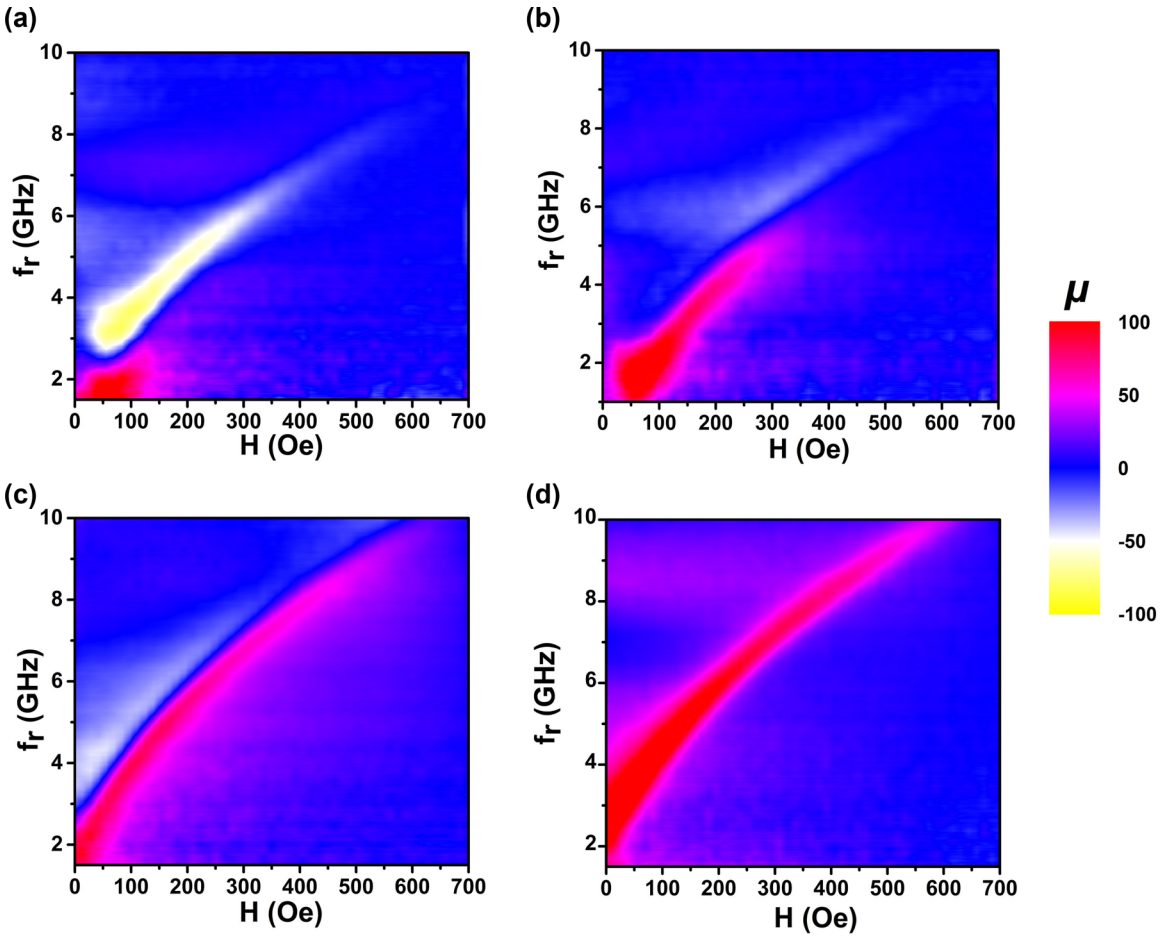

FIG. 4. (a) Real part of Co layer on PMN-PT substrate. Red (yellow) color indicates positive (negative) amplitude. The dashed line corresponds to the plot of the real part of the permeability against frequency shown in Fig. 1(d). (b) Imaginary part of Co layer on PMN-PT substrate; (c) and (d) real and imaginary parts of Co layer on Si substrate. Red (yellow) color indicates positive (negative) amplitude.

is sufficient evidence of the ferroelectric control of magnetic permeability in FE/FM heterostructures. It is unraveled that the magnetic permeability and dielectric permittivity of the FM/FE system, rather than the magnetic moment and electric polarization, are crucial to the dynamic magnetoelectric response of multiferroic FM/FE heterostructures. The results are expected to provide an ideally ultralow power and highly localized method of manipulating magnetization dynamics. For thin FM metal films, the dynamic response of the direct ME effect is limited by the electric field screening and the *s-d* exchange time ($\sim 10^{-15}$ s), which could give rise to a fast magnetization switching in the subpicosecond range. Beyond spintronic applications, our research illustrates how FE/FM multiferroic structures with electric field controllable magnetic permeability can be tailored to provide the requisite refraction index to make them excellent candidates for many exciting optical functionalities, such as electro-optical modulators and nanoscale metamaterials.

This work is supported by the National Basic Research Program of China (Grant No. 2012CB933101), the National Natural Science Foundation of China (Grants No. 11674143, No. 51671099, and No. 11474138), the Program for Changjiang Scholars and Innovative Research Team in University (No. IRT-16R35), and the Fundamental Research Funds for the Central Universities.

[1] T. Yaroslav, A. Brataas, G. E. W. Bauer, and B. I. Halperin, Rev. Mod. Phys. **77**, 1375 (2005).
[2] A. Brataas, A. D. Kent, and H. Ohno, Nat. Mater. **11**, 372 (2012).
[3] X. L. Qi and S. C. Zhang, Rev. Mod. Phys. **83**, 1057 (2011).
[4] P. Dai, J. Hu, and E. Dagotto, Nat. Phys. **8**, 709 (2012).
[5] Y. G. Ma, C. K. Ong, T. Tyc, and U. Leonhardt, Nat. Mater. **8**, 639 (2009).
[6] V. M. Shalaev, Nat. Photon. **1**, 41 (2007).
[7] D. R. Smith, J. B. Pendry, and M. C. Wiltshire, Science **305**, 788 (2004).
[8] O. Acher and A. L. Adenot, Phys. Rev. B **62**, 11324 (2000).
[9] X. L. Fan, D. S. Xue, M. Lin, Z. M. Zhang, D. W. Guo, C. J. Jiang, and J. Q. Wei, Appl. Phys. Lett. **92**, 222505 (2008).
[10] S. F. Zhang and S. S. L. Zhang, Phys. Rev. Lett. **102**, 086601 (2009).
[11] T. L.Gibert, IEEE Trans. Magn. **40**, 3443 (2004).
[12] M. Liu, and N. X. Sun, Philos. Trans. R. Soc. A **372**, 20120439 (2014).
[13] O. Mosendz, J. E. Pearson, F. Y. Fradin, G. E. W. Bauer, S. D. Bader, and A. Hoffmann. Phys. Rev. Lett. **104**, 046601 (2010).
[14] J. C. Slonczewski, Phys. Rev. B **71**, 024411 (2005).
[15] X. Waintal and O. Parcollet, Phys. Rev. Lett. **94**, 247206 (2005).
[16] Y. Shiota, T. Nozaki, F. Bonell, S. Murakami, T. Shinjo, and Y. Suzuki, Nat. Mater. **11**, 39 (2011).
[17] Y. Shiota, S. Miwa, T. Nozaki, F. Bonell, N. Mizuochi, T. Shinjo, H. Kubota, S. Yuasa, and Y. Suzuki, Appl. Phys. Lett. **101**, 102406 (2012).
[18] Y. Shiota, S. Miwa, S. Tamaru, T. Nozaki, H. Kubota, A. Fukushima, Y. Suzuki, and S. Yuasa, Appl. Phys. Lett. **105**, 192408 (2014).
[19] A. M. Deac, A. Fukushima, H. Kubota, H. Maehara, Y. Suzuki, S. Yuasa, Y. Nagamine, K. Tsunekawa, D. D. Djayaprawira, and N. Watanabe, Nat. Phys. **4**, 803 (2008).
[20] C. L. Jia, T. L. Wei, C. J. Jiang, D. S. Xue, A. Sukhov, and J. Berakdar, Phys. Rev. B **90**, 054423 (2014).
[21] C. L. Jia, F. L. Wang, C. J. Jiang, J. Berakdar, and D. S. Xue, Sci. Rep. **5**, 11111 (2015).
[22] Y. J. Li, C. J. Jiang, D. S. Xue, J. Berakdar, and C. L. Jia (unpublished).
[23] S. Engelbrecht, A. M. Shuvaev, Y. Luo, V. Moshnyaga, and A. Pimenov, Europhys. Lett. **95**, 37005 (2011).
[24] Y. Liu, L. F. Chen, C. Y. Tan, H. J. Liu, and C. K. Ong, Rev. Sci. Instrum. **76**, 063911 (2005).
[25] N. X. Sun, and G. Srinivasan, Spin **02**, 1240004 (2012).
[26] C. A. Vaz, J. Hoffman, C. H. Ahn, and R. Ramesh, Adv. Mater. **22**, 2900 (2010).
[27] R. O. Cherifi, V. Ivanovskaya, L. C. Phillips, A. Zobelli, I. C. Infante, E. Jacquet, V. Garcia, S. Fusil, P. R. Briddon, N. Guiblin, A. Mougin, A. A. Ünal, F. Kronast, S. Valencia, B. Dkhil, A. Barthélémy, and M. Bibes, Nat. Mater. **13**, 345 (2014).
[28] M. Liu, J. Hoffman, J. Wang, J. X. Zhang, B. N. Cheeseman, and A. Bhattacharya, Sci. Rep. **3**, 1876 (2013).
[29] F. L. Wang, C. Zhou, C. Zhang, C. H. Dong, C. C. Yang, C. J. Jiang, C. L. Jia, and D. S. Xue, Appl. Phys. Lett. **105**, 062407 (2014).
[30] T. R. Shrout, Z. P. Chang, N. Kim, and S. Markgraf, Ferroelectr. Lett. Sect. **12**, 63 (1990).
[31] See Supplemental Material at http://link.aps.org/supplemental/10.1103/PhysRevB.97.060408 for a more detailed investigation of the imaginary permeability/susceptibility.